Hindawi
Advances in Materials Science and Engineering
Volume 2018, Article ID 5910560, 7 pages
https://doi.org/10.1155/2018/5910560

Research Article

Preparation of Porous Materials by Magnesium Phosphate Cement with High Permeability

Lai Zhenyu, Hu Yang, Fu Xiaojie, Lu Zhongyuan, and Lv Shuzhen

State Key Laboratory of Environment-Friendly Energy Materials, School of Materials Science and Engineering, Southwest University of Science and Technology, Mianyang 621010, China

Correspondence should be addressed to Lai Zhenyu; laizhenyu@swust.edu.cn

Received 10 April 2018; Revised 29 June 2018; Accepted 5 August 2018; Published 9 September 2018

Academic Editor: Claude Estournès

High permeability and strength magnesium phosphate cement (MPC) with porosity, average pore size, and compressive strength varied from 63.2% to 74%, 138.7 μm to 284.7 μm and 2.3 MPa to 4.7 MPa, respectively, were successfully prepared by combining the physical foaming method and chemically entrained gas method at room temperature. The effects of borax content, chemical foaming agent content, zinc powder content and W/S ratio on the porosity, pore size distribution, compressive strength, and permeability of the MPC were investigated. The results indicate that the chemical foaming agent content tends to have little impact on the porosity and compressive strength, and the zinc powder content has the most significant influence on the average pore size of MPC. The air pores distribution and connectivity of MPC were mainly controlled by the borax content, W/S ratio, and chemical foaming agent content. Zinc powder played a destructive role in the pores formed by the early physical foaming and led to an increase in pore size and a large number of through pores, which increased the permeability of the materials.

1. Introduction

Cement-based foam material has high heat capacity, excellent fire resistance, and low cost and is usually used in building energy efficient materials because of its lightweight and thermal insulation properties [1, 2]. It has also been widely applied in acoustic insulation [3, 4], electromagnetic wave absorbing material [5], and safety block material [6]. In recent years, magnesium phosphate cement has also been developed to prepare porous materials to obtain foamed concrete for cast-in-situ construction and high-temperature resistance of cement-based porous materials [7].

Phosphate cement is fabricated by an acid-based solution reaction between a divalent or trivalent oxide and an acid phosphate or phosphoric acid [8–10]. The phosphate used in this system is potassium dihydrogen phosphate, sodium dihydrogen phosphate, or ammonium dihydrogen phosphate. The metal oxides often used are magnesium, aluminum, zinc, and calcium oxides, and magnesium oxide is the most common oxide to prepare magnesium phosphate cement (MPC) [11]. In this reaction, a phosphate gel was formed as a precursor of the ceramics since the metal oxide dissolved to release cations reacted with the hydrolytic phosphate ions, and the main final phase of hydration product is struvite, but many other phases also existed during or after hydration reaction, such as dittmarite ($NH_4MgPO_4{\cdot}H_2O$), schertelite ($(NH_4)_2Mg(HPO_4)_2{\cdot}4H_2O$), newberyite ($MgHPO_4{\cdot}3H_2O$), and magnesium phosphate hydrate $Mg_3(PO_4)_2{\cdot}4H_2O$ [12, 13]. With the in-depth research of MPC, MPC has received an astonishing amount of attention since it was discovered in the nineteenth century [14, 15]. Due to its series of advantages, such as rapid setting, high early strength, strong bonding strength, excellent biocompatibility, and low drying shrinkage, it has been widely used in biomedical fields, civil engineering repair, and stabilization of nuclear or heavy metal [16–21]. Recently, the preparation of porous MPC was reported in some studies such as that of Li and Chen, who prepared a new type of MPC with a density ranging from 210 to 380 kg/m^3 and compressive strength ranging from 1.0 to 2.8 MPa by a prefoaming method [22]. Liu et al. also fabricated MPC with a maximum compressive strength of 0.30 ± 0.05 MPa

and porosity of 83.75% by the physical foaming process [23]. Ma and Chen [7] also obtained a novel foamed concrete with the characteristics of quick setting and high early-strength by using sodium bicarbonate as a foaming agent. However, imperviousness and low strength are the dominant properties of MPC fabricated by the preforming method mentioned above. Recently, the application of cement-based porous materials for hazardous wastewater, such as heavy metals and the radioactive nucleus has attracted more and more attention [24, 25]. Unlike the applications mentioned above, adsorbent materials require good permeability and high strength to form self-supporting systems, thus achieving good service performance.

In this study, magnesium phosphate cement is used as the base material, and porous materials with high water permeability and strength will be prepared by combining the physical foaming method and chemically entrained gas method, using a chemical foaming agent (CF) and zinc powder as the compound foaming agent. Additionally, the effects of borax content, CF content, zinc powder content, and the water to solid ratio (W/S) on the pore size distribution, connectivity, and compressive strength of the MPC were systematically investigated.

2. Materials and Experiments

In the current work, the raw materials for the MPC formation were dead-burnt magnesia (MgO, Liaoning Xinrong Mining Co., Ltd., China) obtained by calcinating magnesium carbonate at 1700°C, and analytically pure ammonium dihydrogen phosphate (ADP, AR-grade, Jinshan Chemical Reagent Co., Ltd., Chengdu, China) and quartz powders were prepared by ball-milling quartz for 30 min. The chemical foaming agent (CF, the primary chemical composition is sodium dodecyl sulfate, alkyl amido betaine, and citric acid) having weak acidity was prepared by our lab, which was combined with zinc powder (Zn) for use as a compound foaming agent. Borax ($Na_2B_4O_7{\cdot}10H_2O$) and analytically pure citric acid monohydrate (CAM) were used as a retarder in this study. As characterized by a laser particle size analyzer, the mean particle diameters of the MgO, ADP, and quartz powders are 29 μm, 60 μm, and 20 μm, respectively. The formulas for fabricating MPC are listed in Table 1, where M/P, M/Q, and Zn/CAM represent the mass ratio of MgO to ADP, MgO to quartz powder, and zinc powder to CAM, and the value is 1, 0.5, and 1, respectively. The CF, zinc powder, and CAM were weighed by the mass of all the solid powders, and the mass of borax weighed the MgO. Additionally, all the water used in this work was tap water from the laboratory.

First, the raw materials including MgO powder, ADP powder, quartz powder, and borax were mixed for 1 min in a vertical-axis planetary mixer according to Table 1. Secondly, the CF, CAM, and water were added and stirred for 1 min, and then zinc powder was mixed with them and stirred rapidly for 90 s. Thirdly, the slurry after mixing was cast into steel moulds with a size of 40 mm × 40 mm × 160 mm. Finally, the specimens of MPC were demolded after 2 h and cured in the lab at a temperature of 20 ± 2°C and a relative humidity of 60 ± 5%. It should be pointed out that the CF and CAM were dissolved in water in advance and then added into the mixer. The sample for SEM is prepared by cast slurry into Φ50 mm × 150 mm column steel moulds, cured at a temperature of 20 ± 2°C and a relative humidity of 60 ± 5% for 28 d, and cut horizontally into five test blocks for analyzing the pore distribution by SEM pictures.

Table 1: The formulas for fabricating MPC.

Sample no.	Borax (%)	CF (%)	Zn (%)	W/S
$M_{I\text{-}1}$	4	1.5	1.0%	0.16
$M_{I\text{-}2}$	7	1.5	1.0%	0.16
$M_{I\text{-}3}$	10	1.5	1.0%	0.16
$M_{II\text{-}1}$	7	1.0	1.0%	0.16
$M_{II\text{-}2}$	7	1.5	1.0%	0.16
$M_{II\text{-}3}$	7	2.0	1.0%	0.16
$M_{III\text{-}1}$	7	1.5	0.5%	0.16
$M_{III\text{-}2}$	7	1.5	1.0%	0.16
$M_{III\text{-}3}$	7	1.5	1.5%	0.16
$M_{IV\text{-}1}$	7	1.5	1.0%	0.14
$M_{IV\text{-}2}$	7	1.5	1.0%	0.16
$M_{IV\text{-}3}$	7	1.5	1.0%	0.18

Before testing porosity, the samples should be dried under the temperature of 60°C for 24 h to obtain a constant weight. The porosity of material was calculated using $P = (1 - (\rho_{\text{apparent}}/\rho_{\text{th}})) \times 100\%$ with an apparent density of the dried material and theoretical density $\rho_{\text{th}} = \sum_{i=1}^{n} v_i \rho_i$ (v_i = volume fraction of component i, ρ_i = density of component i) [26].

The compressive strength of 28 d was applied by a microcomputer control universal testing machine (CMT5105, Shenzhen SANS Testing Machine Co., Ltd., China) with a loading rate of 2.4 kN per second according to standard Chinese GB17671-1999, each sample taken six specimens tested, and the compressive strength is the average value of six samples. Crystal phases were determined by X-ray diffraction using a D/Max-RB (Rigaku, Japan) powder X-ray diffractometer using CuKα irradiation generated at 60 mA and 35 kV; the scanning rate was 8°/min from 3 to 80°. The microstructure of the MPC was observed by scanning electron microscopy (TM1000, Hitachi, Japan), and the distribution of the pore size was determined by analyzing SEM pictures using a soft image analyzer (Nano measurer, China).

3. Results and Discussion

The porosity, average pore size, and compressive strength of the porous MPC fabricated according to Table 1 were measured and the results are listed in Table 2. It can be seen from Table 2 that the porosity increased from 66% to 71.6%, the compressive strength reduced from 4.7 MPa to 2.6 MPa, and the average pore size ranged from 138.7 μm to 160.01 μm as the borax content increased from 4% ($M_{I\text{-}1}$) to 10% ($M_{I\text{-}3}$). This result can be attributed to the retarding effect of borax, which can delay the setting time of MPC slurry. As a result, there is enough time for the air bubbles to expand and migrate in the slurry. As the content of CF increased from

Table 2: Porosity, average pore size, and compressive strength of porous MPC.

Sample no.	Porosity (%)	Average pore size (μm)	Compressive strength (MPa)
$M_{I\text{-}1}$	66 ± 2	139 ± 7	4.7 ± 0.3
$M_{I\text{-}2}$	69 ± 3	160 ± 7	3.3 ± 0.2
$M_{I\text{-}3}$	71 ± 3	155 ± 6	2.6 ± 0.2
$M_{II\text{-}1}$	70 ± 3	141 ± 7	3.2 ± 0.2
$M_{II\text{-}2}$	69 ± 3	160 ± 6	3.3 ± 0.1
$M_{II\text{-}3}$	70 ± 3	180 ± 8	3.2 ± 0.2
$M_{III\text{-}1}$	65 ± 3	152 ± 6	4.6 ± 0.2
$M_{III\text{-}2}$	69 ± 3	160 ± 6	3.3 ± 0.2
$M_{III\text{-}3}$	74 ± 4	285 ± 12	2.3 ± 0.1
$M_{IV\text{-}1}$	63 ± 2	142 ± 7	4.3 ± 0.2
$M_{IV\text{-}2}$	69 ± 3	160 ± 7	3.3 ± 0.2
$M_{IV\text{-}3}$	72 ± 3	200 ± 10	2.5 ± 0.1

1.0% ($M_{II\text{-}1}$) to 2.0% ($M_{II\text{-}3}$), the average pore size rose from 140.6 μm to 180.11 μm, but the porosity and compressive strength remained at about 69% and 3.2 MPa, respectively. As the content of zinc powder and CAM increased from 0.5% to 1.5%, the porosity and average pore size increased from 65.2% to 74% and from 151.9 μm to 284.7 μm, respectively, while the compressive strength decreased from 4.6 MPa to 2.3 MPa. These results may be explained by the reaction between the zinc powder and hydrogen ions which were jointly supplied by the ADP and CAM. The more zinc powder and CAM were added, the more air bubbles were obtained, which led to the higher porosity and lower compressive strength. Furthermore, as the W/S ratio increased from 0.14 to 0.18, the compressive strength reduced from 4.3 MPa to 2.5 MPa due to the porosity and pore diameter size rising from 63.2% to 72%, and from 141.8 μm to 200.4 μm, respectively. The higher W/S ratio makes the consistency of the slurry and foaming resistance lower, which led to a large number of air pores left in the samples and the high porosity obtained.

Figure 1 shows the effect of borax content, CF content, zinc powder content (or CAM content), and W/S ratio on the pore size distribution of the MPC. As shown in Figure 1(a), with the borax content (B%), increased from 4%, 7% to 10%, the pore distribution became wider, ranging from 40 μm to 550 μm, from 80 μm to 1150 μm, and from 70 μm to 1280 μm, respectively. Besides, the majority of pores uniformly ranged from 40 to 300 μm, and the accumulative frequency exceeded 70%. As the content of CF (CF %) increased from 1.0%, 1.5% to 2.0%, the air pore size distribution varied about from 80 μm to 780 μm, 80 μm to 950 μm, and 90 μm to 1280 μm, respectively, as observed from Figure 1(b). However, the CF content has little influence on the smaller air pores, which range in size from 0 to 150 μm. It can be seen from Figure 1(c) that the air pore size distribution ranged from about 0 to 700 μm, from 50 μm to 1300 μm, and from 100 μm to 1350 μm, respectively, as the zinc powder (Zn%) increased from 0.5%, 1.0% to 1.5%. Additionally, a distinct difference can be found that there are about 25% air pores whose size distribution varied from 300 μm to 1350 μm with 1.5% zinc powder in the samples. As seen in Figure 1(d), as the W/S increased from 0.14, 0.16 to 0.18, the size distribution of the air pores varied from 40 to 600 μm, from 50 μm to 1300 μm and from 40 to 750 μm, respectively. Besides, the size of the pores distribution became wider for the specimens with the W/S ratio of 0.16 compared to the other two ratios.

By analyzing the data in Table 2 and Figure 1, there is a certain relationship between the strength of the phosphate cement porous materials and the porosity, pore size of as-prepared materials. In general, the greater the porosity, the lower the strength, and the larger the average pore size, the smaller the strength. But comparing the porosity and average pore size, the effect of porosity is higher than the effect of pore size on the strength; for $M_{II\text{-}1}$, $M_{II\text{-}2}$, and $M_{II\text{-}3}$, the porosity is almost the same, and the average pore size increases from 140 μm to 180 μm, but their strength is maintained at about 3.2 MPa; for $M_{II\text{-}1}$ and $M_{IV\text{-}1}$ with almost the same average pore size of 140 μm, the porosity of $M_{II\text{-}1}$ and $M_{IV\text{-}1}$ is 70.4% and 63.2%, the strength of $M_{II\text{-}1}$ and $M_{IV\text{-}1}$ is 3.2 MPa and 4.3 MPa, and the results indicate that the porosity has a huge influence on the strength. Of course, the foaming agent will also affect the strength. In this paper, zinc powder is used as a chemical foaming material, and the strength of different zinc powders is analyzed, such as $M_{III\text{-}1}$, $M_{III\text{-}2}$, and $M_{III\text{-}3}$ in Table 1, and the strength decreased from 4.6 MPa to 2.3 MPa with increasing amount of Zn. This is due to the increase in the amount of zinc powder, the increase in porosity and the average pore size, and also due to the side effects of zinc on the hydration process [27]. Therefore, for the strength of phosphate cement porous material, the effects are multifaceted, and the influence of porosity plays a leading role than other factors.

Figure 2 shows SEM micrographs of the MPC formulated with different borax content, CF content, zinc powder content, and W/S ratio. As shown in Figures 2(a)–2(c), the size of air pores and the number of connected pores increased obviously when the borax content increased from 4%, 7% to 10%, and the air pores were distributed more uniformly. The pore distribution uniformity and the size of the samples increased slightly as the content of CF increased from 1.0%, 1.5% to 2.0%, but the specimen having the most connected macropores was that with the foaming agent content of 1.5%, as presented in Figures 2(d)–2(f). As can be seen in Figures 2(g)–2(i), the size and connectivity of the air pores increased significantly as the zinc powder content increased from 0.5 wt.% to 1.5 wt.%. However, the pores were distributed less uniformly as higher contents of zinc powder were used in the samples. As seen in Figures 2(j)–2(l), the size and uniformity of the pores increased obviously when the W/S ratio increased from 0.14 to 0.18. As shown by the consequence of Figure 2, the size and uniformity of the pores were mainly controlled by the borax content, zinc powder content, and W/S ratio, while the CF content mainly controlled the connectivity of the air pores.

We selected the sample $M_{III\text{-}2}$ for XRD analysis shown in Figure 3. Figure 3 shows that the primary phase is SiO_2, MgO, and $MgNH_4{\cdot}6H_2O$, of which the SiO_2 peak is the strongest, MgO second, and $MgNH_4{\cdot}6H_2O$ the weakest. The main reason is that SiO_2 mainly acts as a filler and does not

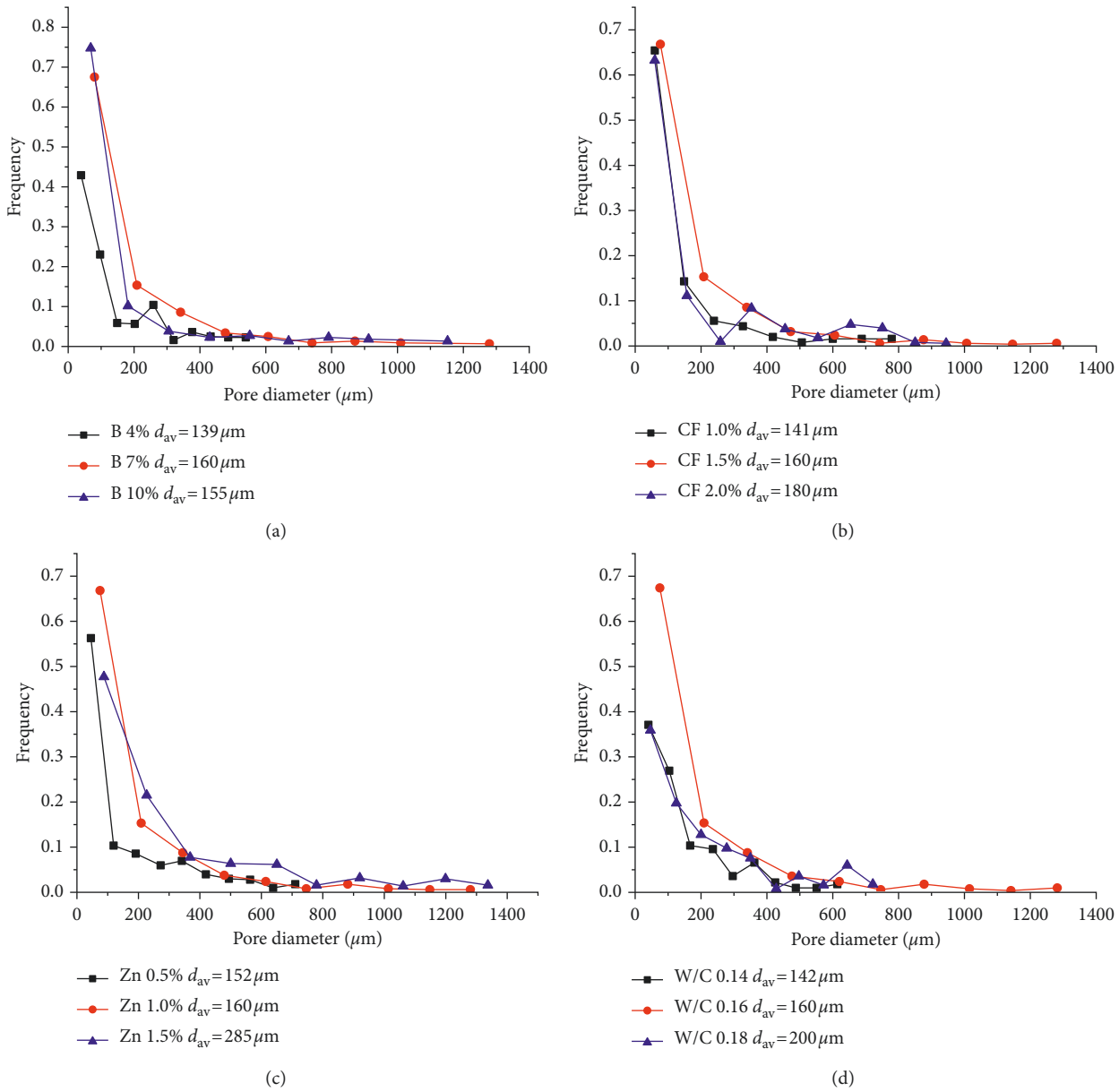

Figure 1: Pore size distribution of porous MPC fabricated with different borax content in (a), varying foaming agent content in (b), varying zinc powder content in (c), and W/S ratios in (d).

participate in the hydration process. Due to the large amount of unreactive SiO_2, the diffraction peaks are sharp. Of course, the incorporation of silica also has more effect. On the one hand, it can prolong the setting time, which is beneficial to the foaming effect of Zn powder and forms more pores, on the other hand, silica can also reduce the hydration heat. The reduction of hydration heat avoids the release of ammonia gas during the reaction, while also avoiding the decomposition of hydration products which leads to the strength loss of the materials [28].

Figure 4 shows the water permeability of MPC fabricated by combining the physical foaming and chemically entrained gas methods. It can be seen that water can pass quickly from the surface to underlying layers of the MPC through the abundant connected pore channels that exist in its interior. In general, permeability is mainly affected by pore size and connectivity of samples. The porous materials obtained by composite foaming technology have a large number of connected pores and large pore size, which can ensure wastewater to easily pass through when used as adsorbent materials.

This paper mainly uses zinc powders as the foaming agent. The previous study also showed that the use of zinc powder could form a better closed-hole structure which has been discussed more detailed, and zinc powder content, water to cement ratio, and borax content play a role on the formation and growth of foams [29]. The chemical medium used in this paper is a weak acid foaming agent, which is to reduce its effect on the slurry of magnesium phosphate cement due to the acidic environment of the initial

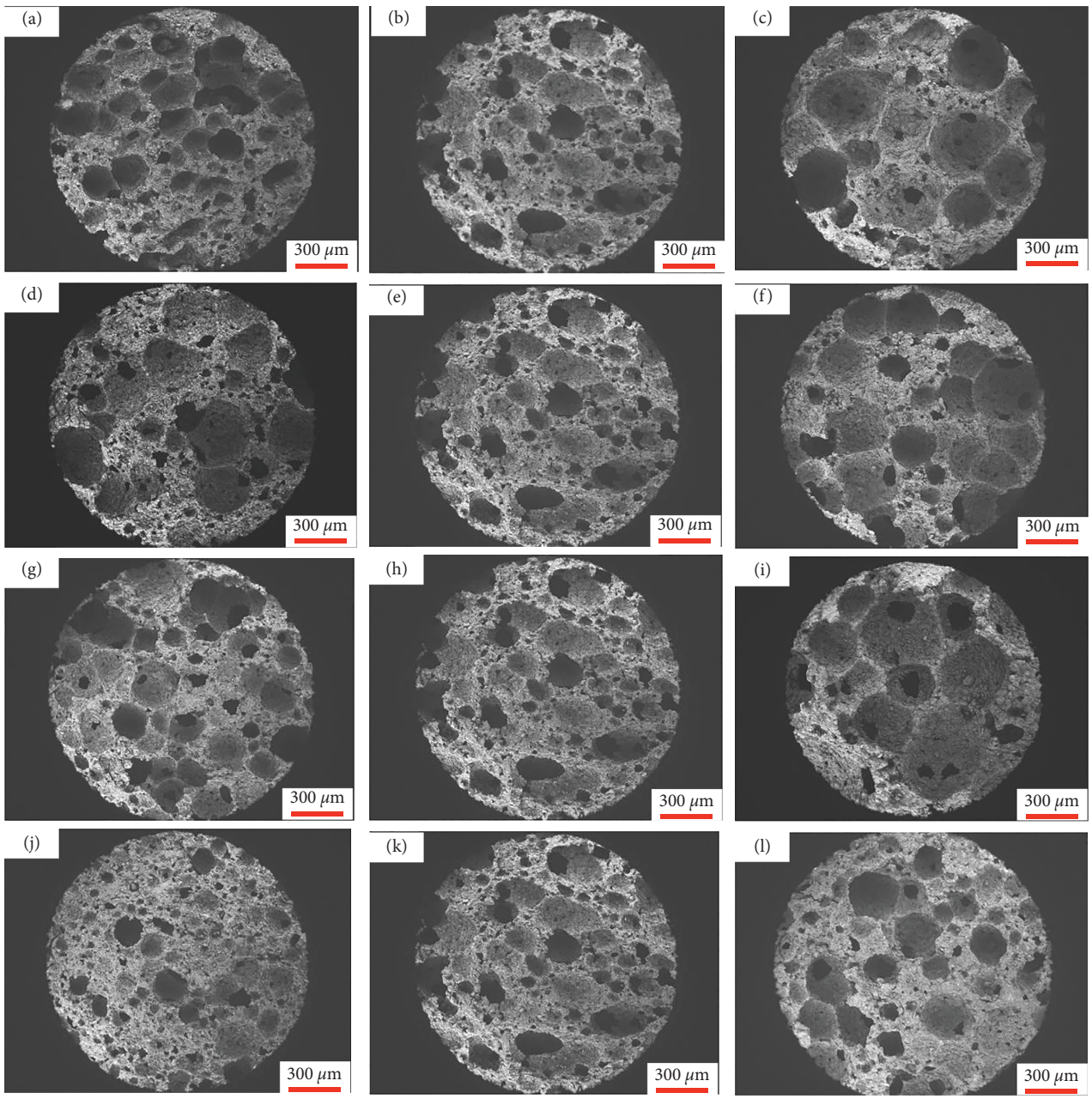

Figure 2: SEM micrographs of the porous MPC with borax contents of 4% in (a), 7% in (b), and 10% in (c); with CF contents of 1.0% in (d), 1.5% in (e), and 2.0% in (f); with zinc powder contents of 0.5% in (g), 1.0% in (h), and 1.5% in (i); and with W/S ratios of 0.14 in (j), 0.16 in (k), and 0.18 in (l).

hydration and to ensure that its strength has no significant loss. In the initial stage of molding, a large number of micropores were formed during the stirring process due to the action of the foaming agent CF. At this time, the effect of zinc powder foaming was not apparent. In the static stage, due to the acidic environment at the initial stage of the phosphate cement reaction, together with the low viscosity in the early stage of hydration, the silica fillers prolonged the hydration hardening time, and the zinc foaming effect was exerted. However, at this time, the zinc powder is mainly located on the pore wall formed in the earlier stage. Therefore, during the foaming process, the pores formed in the early stage were damaged and enlarged, and a large number of through-holes are formed in the structure so that the water permeability of the material is significantly increased.

4. Conclusion

In the present work, magnesium phosphate cement (MPC) with high permeability and strength was successfully fabricated by combining the physical foaming method and chemically entrained gas method at room temperature. The porosity, average pore size, and compressive strength of

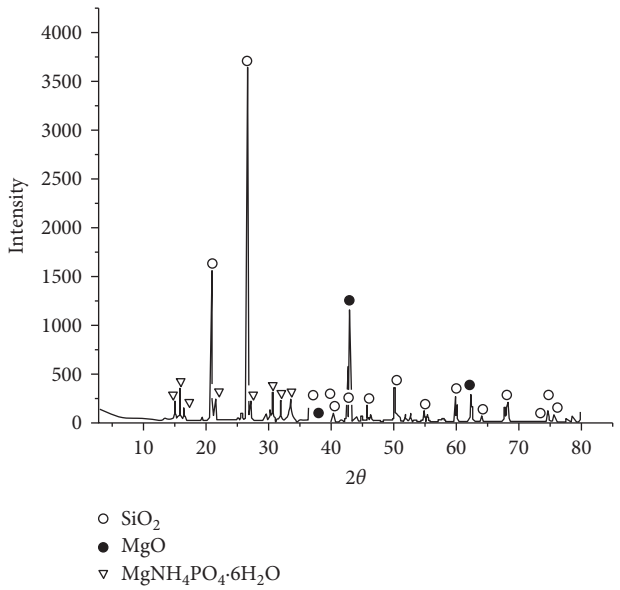

Figure 3: XRD pattern of the sample $M_{III\text{-}2}$.

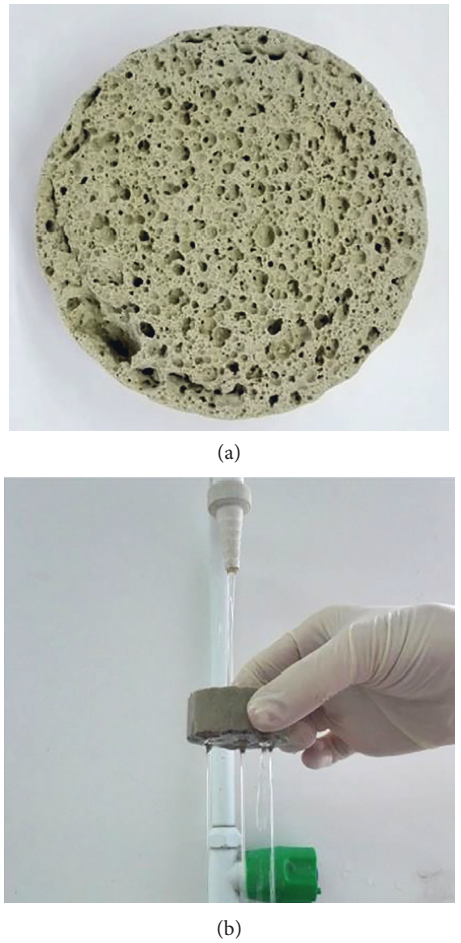

(a)

(b)

Figure 4: Water permeability of porous MPC.

MPC prepared with different formulas ranged from 63.2% to 74%, 138.7 μm to 284.7 μm, and 2.3 MPa to 4.7 MPa, respectively. The content of chemical foaming agent (CF) has little influence on the porosity and compressive strength of specimens. The pore size distribution is significantly influenced by the zinc powder content and W/S ratio. The compressive strength is affected by the borax content, zinc powder content, and W/S ratio. Additionally, MPC with higher porosity and larger pore diameter shows high permeability due to the mass of through pores existing in the samples. As a result, the porous MPC has enormous potential for filtration applications, such as heavy metals, radioactive waste, exhaust fumes, and could also be used for bio-scaffolds in tissue engineering.

Data Availability

The data used to support the findings of this study are available from the corresponding author upon request.

Conflicts of Interest

The authors declare that they have no conflicts of interest.

Acknowledgments

The authors would like to acknowledge funding from key R&D project of Sichuan Province (2018GZ0148) and Southwest University of Science and Technology (13zxfk04 and 14tdfk01).

References

[1] G. Sang, Y. Zhu, G. Yang, and H. Zhang, "Preparation and characterization of high porosity cement-based foam material," *Construction and Building Materials*, vol. 91, pp. 133–137, 2015.

[2] Q. Zeng, M. Luo, X. Pang, L. Li, and K. Li, "Surface fractal dimension: an indicator to characterize the microstructure of cement-based porous materials," *Applied Surface Science*, vol. 282, pp. 302–307, 2013.

[3] H. K. Kim and H. K. Lee, "Influence of cement flow and aggregate type on the mechanical and acoustic characteristics of porous concrete," *Applied Acoustics*, vol. 71, no. 7, pp. 607–615, 2010.

[4] J. Olek, W. J. Weiss, N. Neithalath, A. Marolf, E. Sell, and W. D. Thornton, *Development of Quiet and Durable Porous Portland Cement Concrete Paving Materials*, Final Report SQDH 2003-5, Purdue University, West Lafayette, IN, USA, 2003.

[5] J. H. Ha, S. Lee, J. R. Choi, J. Lee, I. Song, and T. J. Chung, "A self-setting particle-stabilized porous ceramic panel prepared from commercial cement and loaded with carbon for potential radar-absorbing applications," *Processing and Application of Ceramics*, vol. 12, no. 1, pp. 86–93, 2018.

[6] X. Luo, J. Xu, E. Bai, and W. Li, "Mechanical properties of ceramics–cement based porous material under impact loading," *Materials & Design*, vol. 55, pp. 778–784, 2014.

[7] C. Ma and B. Chen, "Experimental study on the preparation and properties of a novel foamed concrete based on magnesium phosphate cement," *Construction and Building Materials*, vol. 137, pp. 160–168, 2017.

[8] M. Morales, J. Formosa, E. Xuriguera et al., "Elastic modulus of a chemically bonded phosphate ceramic formulated with

low-grade magnesium oxide determined by nano-indentation," *Ceramics International*, vol. 41, no. 9, pp. 12137–12146, 2015.

[9] I. Odler, *Special Inorganic Cements, Modern Concrete Technology Series*, Taylor & Francis, London, UK, 2000.

[10] E. Soudée and J. Pera, "Mechanism of setting reaction in magnesia-phosphate cements," *Cement and Concrete Research*, vol. 30, no. 2, pp. 315–321, 2000.

[11] A. Wang, J. Zhang, J. Li et al., "Effect of liquid-to-solid ratios on the properties of magnesium phosphate chemically bonded ceramics," *Materials Science and Engineering: C*, vol. 33, no. 5, pp. 2508–2512, 2013.

[12] J. Formosa, J. M. Chimenos, A. M. Lacasta, and M. Niubó, "Interaction between low-grade magnesium oxide and boric acid in chemically bonded phosphate ceramics formulation," *Ceramics International*, vol. 38, no. 3, pp. 2483–2493, 2012.

[13] A. S. Wagh, *Chemically Bonded Phosphate Ceramics: Twenty-First Century Materials with Diverse Applications*, Elsevier, Amsterdam, Netherlands, 2016.

[14] A. S. Wagh, "Recent progress in chemically bonded phosphate ceramics," *ISRN Ceramics*, vol. 2013, Article ID 983731, 20 pages, 2013.

[15] D. A. Hall, R. Stevens, and B. El-Jazairi, "The effect of retarders on the microstructure and mechanical properties of magnesia–phosphate cement mortar," *Cement and Concrete Research*, vol. 31, no. 3, pp. 455–465, 2001.

[16] A. Wang, Z. Yuan, J. Zhang et al., "Effect of raw material ratios on the compressive strength of magnesium potassium phosphate chemically bonded ceramics," *Materials Science and Engineering: C*, vol. 33, no. 8, pp. 5058–5063, 2013.

[17] B. Xu, H. Ma, and Z. Li, "Influence of magnesia-to-phosphate molar ratio on microstructures, mechanical properties and thermal conductivity of magnesium potassium phosphate cement paste with large water-to-solid ratio," *Cement and Concrete Research*, vol. 68, pp. 1–9, 2015.

[18] Q. Yang, B. Zhu, S. Zhang, and X. Wu, "Properties and applications of magnesia–phosphate cement mortar for rapid repair of concrete," *Cement and Concrete Research*, vol. 30, no. 11, pp. 1807–1813, 2000.

[19] H. Ma, B. Xu, Y. Lu, and Z. Li, "Modeling magnesia-phosphate cement paste at the micro-scale," *Materials Letters*, vol. 125, pp. 15–18, 2014.

[20] H. Ma, B. Xu, and Z. Li, "Magnesium potassium phosphate cement paste: degree of reaction, porosity and pore structure," *Cement and Concrete Research*, vol. 65, pp. 96–104, 2014.

[21] A. S. Wagh, S. Y. Jeong, D. Singh, R. Strain, H. No, and J. Wescott, "Stabilization of contaminated soil and wastewater with chemically bonded phosphate ceramics," in *Proceedings of Waste Management 1997 (WM'97)*, Tucson, AZ, USA, 1997.

[22] Y. Li and B. Chen, "New type of super-lightweight magnesium phosphate cement foamed concrete," *Journal of Materials in Civil Engineering*, vol. 27, no. 1, article 04014112, 2014.

[23] L. J. Liu, J. H. Li, X. Wang et al., "Tailoring the strength and porosity of rapid-hardening magnesia phosphate paste via the pre-foaming method," *Scientific Reports*, vol. 5, no. 1, article 13016, 2015.

[24] M. Masanobu, S. Yoshimasa, H. Naoko et al., "Adsorptivity of heavy metals CuII, CdII, and PbII on woodchip-mixed porous mortar," *Chemical Engineering Journal*, vol. 215-216, pp. 202–208, 2013.

[25] A. P. Varlakov and A. V. Germanov, "Organic radiowaste immobilization by permeation of porous cement matrices," *Atomic Energy*, vol. 113, no. 2, pp. 100–105, 2012.

[26] F. K. Juillerat, U. T. Gonzenbach, and L. J. Gauckler, "Tailoring the hierarchical pore structures in self-setting particle-stabilized foams made from calcium aluminate cement," *Materials Letters*, vol. 70, pp. 152–154, 2012.

[27] Z. Lai, X. Lai, J. Shi, and Z. Lu, "Effect of Zn^{2+} on the early hydration behavior of potassium phosphate based magnesium phosphate cement," *Construction and Building Materials*, vol. 129, pp. 70–78, 2016.

[28] C. You, J. Qian, J. Qin, H. Wang, Q. Wang, and Z. Ye, "Effect of early hydration temperature on hydration product and strength development of magnesium phosphate cement (MPC)," *Cement and Concrete Research*, vol. 78, pp. 179–189, 2015.

[29] X. J. Fu, Z. Y. Lai, X. C. Lai, Z. Y. Lu, and S. Z. Lv, "Preparation and characteristics of magnesium phosphate cement based porous materials," *Construction and Building Materials*, vol. 127, pp. 712–723, 2016.